Available online at www.sciencedirect.com
SCIENCE DIRECT®
Journal of Solid State Chemistry 177 (2004) 3581–3589
JOURNAL OF SOLID STATE CHEMISTRY
http://elsevier.com/locate/jssc

The anionic 3D-framework $[Ga_2(PO_4)_3]_\infty$: a microporous host lattice for various species

J. Lesage,[a] A. Guesdon,[a,*] B. Raveau,[a] and Vaclav Petricek[b]

[a] *Laboratoire de Cristallographie et Sciences des Materiaux, Ecole Nationale Superieure d'Ingenieurs de Caen, CNRS ENSICAEN-UMR 6508, 6 boulevard Maréchal Juin, 14050 Caen Cedex, France*
[b] *Institute of Physics ASCR, Na Slovance 2, 182 21 Praha 8, Czech Republic*

Received 19 March 2004; received in revised form 10 June 2004; accepted 15 June 2004

Available online 12 August 2004

Abstract

The structure of $(NH_4)_3Ga_2(PO_4)_3$ has been revisited from a single crystal X-ray diffraction study. The detailed description of the microporous $[Ga_2(PO_4)_3]_\infty$ framework of this phosphate shows that it is in fact an intersecting tunnel structure and that the lattice of NH_4^+ cations forms rows of edge-shared tetrahedra. Moreover, the positions of hydrogen atoms are determined, allowing the hydrogen bonds to be evidenced. The possibility of substitution of Rb^+ and Cs^+ cations for NH_4^+ in one N(1) site is demonstrated. An additional analysis of the structure of the previously obtained phosphates $(NH_4)[M(H_2O)_2]Ga_2(PO_4)_3$ with M = Co, Mn shows that the latter possess the same $[Ga_2(PO_4)_3]_\infty$ microporous framework which accommodates $MO_4(H_2O)_2$ octahedra instead of NH_4^+ cations.

Keywords: Ammonium gallium monophosphate; Hydrothermal synthesis; Single crystal; X-ray diffraction; Structure determination; Tunnel structure; Hydrogen bonds; Three-dimensional host lattice; Cationic substitution

1. Introduction

Gallium phosphates, because of their similarity with aluminum phosphates, have been the subject of numerous studies these last 10 years. Several microporous gallium phosphates were indeed discovered [1–5] using organic agents as templates. Most of these host frameworks involve OH groups or H_2O molecules so that they are not really pure oxides. But on the other hand, attempts to prepare gallium phosphates using large alkali cations do not allow generally large tunnels to be obtained. In this respect, the recent discovery of the gallophosphate $(NH_4)_3Ga_2(PO_4)_3$, called 3D-GAPON by Bonhomme et al. [6] is of high interest. The X-ray powder structure study of this oxide carried out by these authors shows that its $[Ga_2(PO_4)_3]_\infty$ 3D framework exhibits very spacious elliptic but constricted channels. We have revisited this system using different conditions for synthesis. We describe herein the synthesis and crystal growth of $(NH_4)_3Ga_2(PO_4)_3$ using hydrothermal synthesis. The single crystal structure redetermination provides more accurate coordinates, and in particular localization of hydrogen atoms so that a more detailed description of the structure can be proposed. A possibility of partial substitution of univalent cations NH_4^+ by Rb^+ and Cs^+ is studied as well, and the structures of single crystals of general formula $(NH_4)_{3-x}A_xGa_2(PO_4)_3$ (A = Rb and Cs) were determined for x ranging from 0.23 to 0.54. It has been shown that the $[Ga_2(PO_4)_3]_\infty$ framework is practically not affected by the substitution. Finally, the comparison of these structures with that of the phosphates $(NH_4)[M(H_2O)_2]Ga_2(PO_4)_3$ with M = Co, Mn [7,8] leads to the conclusion that all this series of oxides possess the same host lattice $[Ga_2(PO_4)_3]_\infty$ remaining practically unaffected by the nature of the interpolated species: NH_4^+, Cs^+, Rb^+, Co^{2+} or Mn^{2+} with H_2O.

2. Synthesis and crystal growth

Crystals of $(NH_4)_3Ga_2(PO_4)_3$ were obtained under hydrothermal conditions using 21 mL Teflon-lined stainless steel Parr autoclaves. Ga_2O_3 (Alfa Aesar

*Corresponding author. Fax: +33-2-31-95-16-00.
E-mail address: anne.guesdon@ismra.fr (A. Guesdon).

0022-4596/$ - see front matter © 2004 Elsevier Inc. All rights reserved.
doi:10.1016/j.jssc.2004.06.024

99.9%) and $(NH_4)_2HPO_4$ (Prolabo Rectapur 99%) were ground in an agate mortar in the molar ratio Ga:P = 2:3. Approximately 0.4 mL of deionized water was then added to 0.8 g of the phosphate–oxide mixture, leading to a highly viscous solution. Its pH was calculated to be slightly basic, i.e., 8.1. The so obtained solution was heated in the autoclave at 180°C for 25 h and finally slowly cooled at room temperature for 18 h. Colorless crystals were thus obtained mixed with whitish powder. They were separated from the solution by vacuum filtration, washed with deionized water and dried in air. Note that the final solution turned basic during the reaction (pH ~ 11). X-ray pattern analysis (pattern registered with a PHILIPS PW 1830 diffractometer using the Cu$K\alpha$ radiation) showed that three phases are present under these conditions: Ga_2O_3, $(NH_4)_3Ga_2(PO_4)_3$ [6] and $(NH_4)Ga(PO_4)OH$ [6]. Remarking that the formation of $(NH_4)Ga(PO_4)OH$ is related to basic conditions of synthesis, we tried to buffer our solution using both $(NH_4)_2HPO_4$ and H_3PO_4 (85%) (Prolabo Rectapur) in the molar ratio 2:1, keeping the Ga:P molar ratio at 2:3. In these conditions, the pH (calculated value: 6.9) remained neutral at the end of the reaction and we did not detect the phase $(NH_4)Ga(PO_4)OH$ anymore. Nevertheless, a small amount of starting gallium oxide was always observed in X-ray powder patterns, even when the molar ratio Ga:P was increased up to 2:15. The synthesis of the crystals $(NH_4)_{3-x}A_xGa_2(PO_4)_3$ with A = Rb, Cs was performed in the same way, but adding ANO_3 nitrates (Chempur 99.9%). The molar ratio ANO_3:$(NH_4)_2HPO_4$ was 1:1. The expected phases were thus synthesized with the only presence of Ga_2O_3 as secondary phase. Note that the $(NH_4)Ga(PO_4)OH$ phase was never obtained besides the expected phase, whenever $(NH_4)_2HPO_4$ or a mixture of $(NH_4)_2HPO_4$ and H_3PO_4 (85%) were used. Attempts to substitute totally Cs^+ or Rb^+ for NH_4^+ in the same conditions of pH and volume solution (i.e., attempts to prepare $A_3Ga_2(PO_4)_3$ compounds) were unsuccessful. Note that the synthesis of the title compounds is quite difficult to perform in aqueous conditions, as described by Bonhomme et al. [6] who used partially or totally ethylene glycol as solvent in order to have viscous conditions. Increasing the amount of additional water produces indeed leucophosphite-type phases in neutral or slightly acid conditions. Strong acidic conditions lead to $GaPO_4$ while, as noticed above, basic conditions lead to $(NH_4)Ga(PO_4)OH$.

3. X-ray single crystal structure determination

Colorless single crystals of $(NH_4)_3Ga_2(PO_4)_3$ and $Cs_{0.54}(NH_4)_{2.46}Ga_2(PO_4)_3$ were studied with a BRUKER-NONIUS Kappa CCD four-circle diffractometer equipped with a bidimensional CCD detector. The single crystal of $Rb_{0.23}(NH_4)_{2.77}Ga_2(PO_4)_3$ was studied with a CAD4 ENRAF-NONIUS diffractometer. Both of them are fitted with a graphite monochromator and use Mo$K\alpha$ radiation. Data collections were made at 293 K, using the experimental conditions described in Table 1. The cell was determined to be monoclinic for the three phases with cell parameters listed in Table 1. Examination of the collected data showed the following systematic extinctions: $h\,k\,l$: $h+k=2n+1$; $h\,0\,l$: $h, l = 2n+1$; $(0\,k\,0 : k = 2n+1)$, which are consistent with two possible space groups: $C2/c$ and Cc. The structure of the cesium gallophosphate was solved in the centrosymmetric space group $C2/c$ by the heavy atom method and successive Fourier difference synthesis made by Jana2000 [9] to localize all Ga, P and O atoms. For the two other compounds, structures were refined starting from the atomic parameters obtained for $Cs_{0.54}(NH_4)_{2.46}Ga_2(PO_4)_3$.

Hydrogen atoms positions were determined by Fourier difference using the only reflections from the limited range $5.84° \leqslant \theta \leqslant 20.81°$. We did not succeed in localizing H(1) atoms for $(NH_4)_{3-x}A_xGa_2(PO_4)_3$ (A = Cs, Rb), since the N(1) position is partially substituted by Cs(1) or Rb(1). In these two crystals, the sum of occupancies of this site was restrained to be equal to 1 and atomic positions and displacement parameters of the two atoms (N and Cs or Rb) were also restrained to have the same values.

All the atomic displacement parameters were refined anisotropically, except for hydrogen atoms which were restrained to have the same isotropic displacement parameter. Absorption and secondary extinction corrections were applied. The atomic parameters for three studied compounds are listed in Table 2.

Further details of the crystal structure investigations (including anisotropic displacement parameters and Fo–Fc lists) can be obtained from the Fachinformationszentrum Karlsruhe, 76344 Eggenstein-Leopoldshafen, Germany (fax: (49) 7247-808-666; e-mail: crysdata@fiz.karlsruhe.de), on quoting the following depositary numbers: CSD-413870 for $Rb_{0.23}(NH_4)_{2.77}Ga_2(PO_4)_3$, CSD-413871 for $Cs_{0.54}(NH_4)_{2.46}Ga_2(PO_4)_3$ and CSD-413872 for $(NH_4)_3Ga_2(PO_4)_3$.

4. Results and discussion

The single crystal structure determination of the pure ammonium phosphate confirmed the structure previously obtained for the composition $(NH_4)_3Ga_2(PO_4)_3$ [6]. The $[Ga_2P_3O_{12}]_\infty$ framework is indeed built up of corner-shared GaO_5 bipyramids and PO_4 tetrahedra. The projection of this framework along $\vec{c}$ (Fig. 1) shows that the GaO_5 and PO_4 polyhedra form constricted elliptic tunnels running along $\vec{c}$. Moreover, the projections of the structure along the [101] and [10$\bar{1}$]

Table 1
Summary of crystal data, intensity measurements and structure refinement parameters for $(NH_4)_3Ga_2(PO_4)_3$, $Rb_{0.23}(NH_4)_{2.77}Ga_2(PO_4)_3$ and $Cs_{0.54}(NH_4)_{2.46}Ga_2(PO_4)_3$

	$(NH_4)_3Ga_2(PO_4)_3$	$Rb_{0.23}(NH_4)_{2.77}Ga_2(PO_4)_3$	$Cs_{0.54}(NH_4)_{2.46}Ga_2(PO_4)_3$
1. Crystal data			
Crystal dimensions (mm^3)	$0.100 \times 0.065 \times 0.050$	$0.180 \times 0.130 \times 0.130$	$0.075 \times 0.050 \times 0.075$
Space group	$C2/c$	$C2/c$	$C2/c$
Cell dimensions	$a = 13.3948(16)$ Å	$a = 13.3782(13)$ Å	$a = 13.392(2)$ Å
	$b = 10.3138(9)$ Å	$b = 10.3260(6)$ Å	$b = 10.3579(9)$ Å
	$c = 9.0361(9)$ Å	$c = 9.0204(7)$ Å	$c = 9.0436(8)$ Å
	$\beta = 111.323(7)^\circ$	$\beta = 111.366(7)^\circ$	$\beta = 111.412(9)^\circ$
Volume (Å^3)	$V = 1162.9(2)$	$V = 1160.46(17)$	$V = 1167.8(2)$
Z	4	4	4
Formula weight ($g\,mol^{-1}$)	478.5	492.0	540.5
ρ_{calc} ($g\,cm^{-3}$)	2.7320(5)	2.8149(4)	3.0731(6)
2. Intensity measurements			
λ(Mo$K\alpha$) (Å)	0.71069	0.71069	0.71069
Scan strategies	φ and ω scans	ω–*2/3*θ	φ and ω scans
	0.8° frame^{-1}	*Scan width*: $1.20 + 0.35 \tan\theta$	0.5° frame^{-1}
	25 s/°	*Split aperture*: $1.20 + \tan\theta$	15 s/°
	2 iterations		2 iterations
	Crystal–detector distance	3 standards reflexions	*Crystal–detector distance*
	$D_x = 36$ mm	Measured every 3600 s	$D_x = 34$ mm
θ range for data collection and limiting indices	$5.84^\circ \leqslant \theta \leqslant 44.32^\circ$	$2.56^\circ \leqslant \theta \leqslant 44.90^\circ$	$5.84^\circ \leqslant \theta \leqslant 42^\circ$
	$-26 \leqslant h \leqslant 26$	$-26 \leqslant h \leqslant 26$	$-25 \leqslant h \leqslant 24$
	$-20 \leqslant k \leqslant 19$	$0 \leqslant k \leqslant 20$	$-19 \leqslant k \leqslant 15$
	$-17 \leqslant l \leqslant 16$	$-17 \leqslant l \leqslant 17$	$-16 \leqslant l \leqslant 17$
Measured reflections	18122	9506	9587
Reflections with $I > 3\sigma$	4589	4758	4060
Independent reflections with $I > 3\sigma$	2573	2741	2339
μ (mm^{-1})	5.114	5.983	6.756
Extinction coefficient g (Type I, Lorentzian)	$0.30.10^{-4}$	$0.10.10^{-4}$	$0.05.10^{-4}$
3. Structure solution and refinement			
Parameters refined	112	107	107
Agreement factors	$R = 0.0291$	$R = 0.0249$	$R = 0.0363$
	$R_w = 0.0260$	$R_w = 0.0275$	$R_w = 0.0366$
Weighting scheme	$w = 1/\sigma^2(F) + 1.10^{-4}F^2)$	$w = 1/\sigma^2(F) + 1.10^{-4}F^2)$	$w = 1/\sigma^2(F) + 1.10^{-4}F^2)$
Δ/σ max	4.67×10^{-2}	4.08×10^{-2}	2.93×10^{-2}

directions (Figs. 2 and 3) show that there exist also large eight-sided tunnels running along those directions that intersect the [001] tunnels. The $[Ga_2P_3O_{12}]_\infty$ framework can be very simply described from undulating $[Ga_2P_2O_{10}]_\infty$ layers interconnected through $[PO_2]_\infty$ layers of isolated PO_4 tetrahedra (Fig. 1). These layers are parallel to the $(\vec{b},\vec{c})$ plane. The projection of such a layer onto the $(\vec{b},\vec{c})$ plane (Fig. 4) shows that it can be described by the assemblage of undulating $[GaPO_7]_\infty$ chains running along $\vec{b}$. Each $[GaPO_7]_\infty$ chain is linked to the next one through the apices of its polyhedra in such a way that the apex of one PO_4 tetrahedron of one chain is shared with one GaO_5 bipyramid of the next chain. Note that such layers form very large eight-sided windows, in agreement with the opened character of the structure. The interatomic distances (Table 3) observed from the single crystal data, although they are similar to those determined previously from powder data [6], show some significant differences. The GaO_5 bipyramid is slightly less distorted than expected from powder data, since the three equatorial distances observed here are slightly larger (1.838–1.849 Å instead of 1.786–1.821 Å) and the apical bonds are smaller or practically equal (1.985–1.988 Å instead of 1.966–2.00 Å). The P(1) tetrahedra, which constitute the $[PO_2]_\infty$ layers of isolated tetrahedra, are practically regular with P–O distances ranging from 1.534 to 1.544 Å. This is in agreement with the fact that their four corners are shared with GaO_5 bipyramids, whereas from powder data they were found to be more distorted (1.550–1.507 Å). The PO_4 tetrahedra P(2), which belongs to the $[GaPO_7]_\infty$ chains, are more distorted, with a shorter P–O bond corresponding to the free apex (1.512 Å, similar to that obtained from powder data 1.514 Å) and three longer one (1.533–1.552 Å, to be compared to 1.531–1.546 Å in powder data). The ammonium cations

Table 2
Positional parameters, atomic displacement parameters, site occupancy and their estimated standard deviations in: (a) $(NH_4)_3Ga_2(PO_4)_3$; (b) $Rb_{0.23}(NH_4)_{2.77}Ga_2(PO_4)_3$; (c) $Cs_{0.54}(NH_4)_{2.46}Ga_2(PO_4)_3$

Atom		x	y	z	U_{eq}. (Å^2)	$N(1)$ occup.
Ga(1)	*a*	0.332048(12)	0.077043(14)	0.419431(16)	0.00649(4)	
	b	0.331661(11)	0.077109(14)	0.419019(16)	0.00763(3)	
	c	0.331402(18)	0.07678(3)	0.41892(3)	0.00661(7)	
P(1)	*a*	0.5	0.00313(5)	0.25	0.00696(13)	
	b	0.5	0.00318(5)	0.25	0.00816(11)	
	c	0.5	0.00449(8)	0.25	0.0071(2)	
P(2)	*a*	0.20626(3)	0.87454(3)	0.16039(4)	0.00798(10)	
	b	0.20591(3)	0.87414(3)	0.16012(4)	0.00902(8)	
	c	0.20666(4)	0.87290(6)	0.16066(6)	0.00786(15)	
O(1)	*a*	0.26364(9)	0.22990(10)	0.33761(12)	0.0124(3)	
	b	0.26302(9)	0.22983(10)	0.33687(13)	0.0133(3)	
	c	0.26144(13)	0.22917(16)	0.33698(18)	0.0114(5)	
O(2)	*a*	0.28247(9)	−0.08222(10)	0.32789(12)	0.0130(3)	
	b	0.28203(9)	−0.08202(10)	0.32766(12)	0.0141(3)	
	c	0.28230(13)	−0.08313(16)	0.32864(18)	0.0122(5)	
O(3)	*a*	0.44845(8)	0.08910(10)	0.60804(12)	0.0118(3)	
	b	0.44854(8)	0.08916(10)	0.60810(11)	0.0129(2)	
	c	0.44869(12)	0.08668(17)	0.60803(17)	0.0112(4)	
O(4)	*a*	0.22955(9)	0.05075(10)	0.52989(12)	0.0116(3)	
	b	0.22899(9)	0.05119(10)	0.52928(12)	0.0131(3)	
	c	0.22984(13)	0.05169(17)	0.53083(18)	0.0108(5)	
O(5)	*a*	0.41935(9)	0.09276(10)	0.28373(12)	0.0113(3)	
	b	0.41915(8)	0.09258(10)	0.28302(12)	0.0126(3)	
	c	0.41873(12)	0.09400(16)	0.28341(18)	0.0107(5)	
O(6)	*a*	0.09030(9)	0.89636(11)	0.13954(15)	0.0199(4)	
	b	0.08973(9)	0.89490(13)	0.13958(16)	0.0208(4)	
	c	0.09015(13)	0.8915(2)	0.1389(2)	0.0190(6)	
N(1)	*a*	0	0.1050(3)	0.25	0.0301(9)	1
N(1)/Rb(1)	*b*	0	0.11822(10)	0.25	0.0324(3)	0.7739(17)
N(1)/Cs(1)	*c*	0	0.12672(4)	0.25	0.01862(13)	0.4618(13)
H(1a)	*a*	0.036(2)	0.048(3)	0.205(3)	0.052(3)	
	b					
	c					
H(1b)	*a*	−0.040(2)	0.152(3)	0.219(4)	0.052(3)	
	b					
	c					
N(2)	*a*	0.38717(13)	0.29546(15)	0.03893(18)	0.0183(5)	
	b	0.38651(12)	0.29471(15)	0.03968(17)	0.0177(4)	
	c	0.38597(18)	0.2958(3)	0.0412(3)	0.0178(7)	
H(2a)	*a*	0.457(2)	0.322(3)	0.062(3)	0.052(3)	
	b	0.460(2)	0.314(3)	0.057(4)	0.051(5)	
	c	0.449(3)	0.319(4)	0.058(4)	0.040(5)	
H(2b)	*a*	0.347(2)	0.358(3)	0.026(3)	0.052(3)	
	b	0.352(3)	0.345(3)	0.038(4)	0.051(5)	
	c	0.347(3)	0.373(4)	0.014(4)	0.040(5)	

Table 2 (*continued*)

Atom		x	y	z	U_{eq}. (Å^2)	$N(1)$ occup.
H(2c)	*a*	0.382(2)	0.252(3)	0.096(3)	0.052(3)	
	b	0.384(2)	0.239(3)	0.139(4)	0.051(5)	
	c	0.379(3)	0.246(4)	0.127(4)	0.040(5)	
H(2d)	*a*	0.365(2)	0.245(3)	−0.044(4)	0.052(3)	
	b	0.362(3)	0.241(3)	−0.038(4)	0.051(5)	
	c	0.356(3)	0.260(4)	−0.043(5)	0.040(5)	

All atoms except hydrogen atoms were refined anisotropically and are given in the form of the isotropic equivalent displacement parameter U_{eq} defined by $U_{eq} = 1/3\sum_{i=1}^{3}\sum_{j=1}^{3} U_{ij}a^{*i}a^{*j}\vec{a}_i\vec{a}_j$.

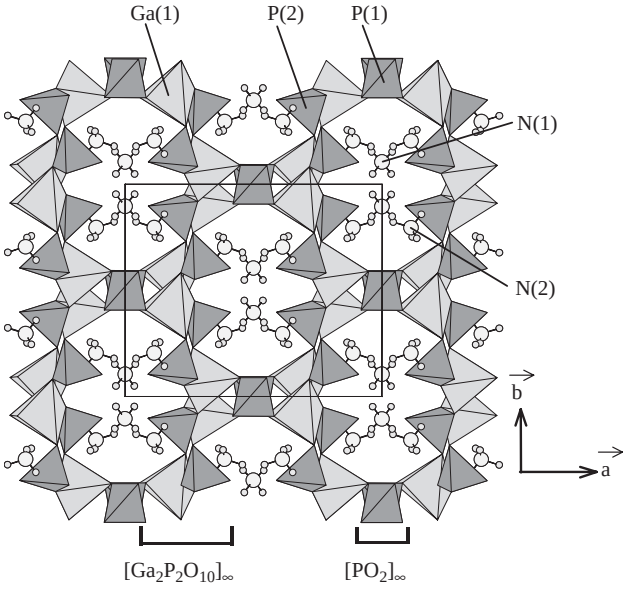

Fig. 1. Projection of the structure of $(NH_4)_3Ga_2(PO_4)_3$ along $\vec{c}$, showing the elliptic constricted tunnels formed by the PO_4 tetrahedra and the GaO_5 bipyramids. The undulating (100) layers $[Ga_2P_2O_{10}]_\infty$ interconnected through isolated PO_4 tetrahedra ($[PO_2]_\infty$ layers) are also shown.

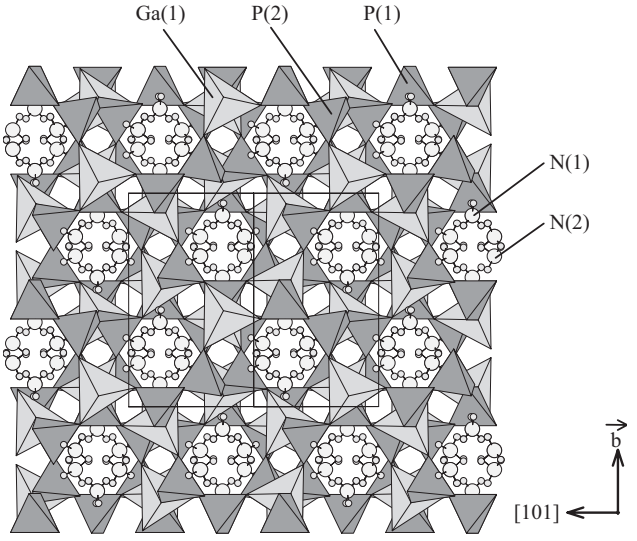

Fig. 3. Projection of the structure of $(NH_4)_3Ga_2(PO_4)_3$ along the $[10\bar{1}]$ direction, showing large eight-sided tunnels running along this direction.

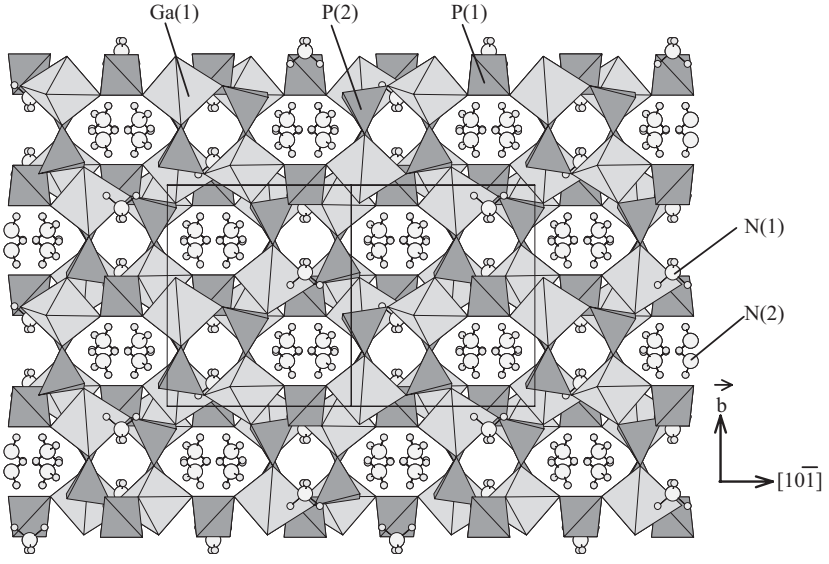

Fig. 2. Projection of the structure of $(NH_4)_3Ga_2(PO_4)_3$ along the [101] direction, showing large eight-sided tunnels running along this direction.

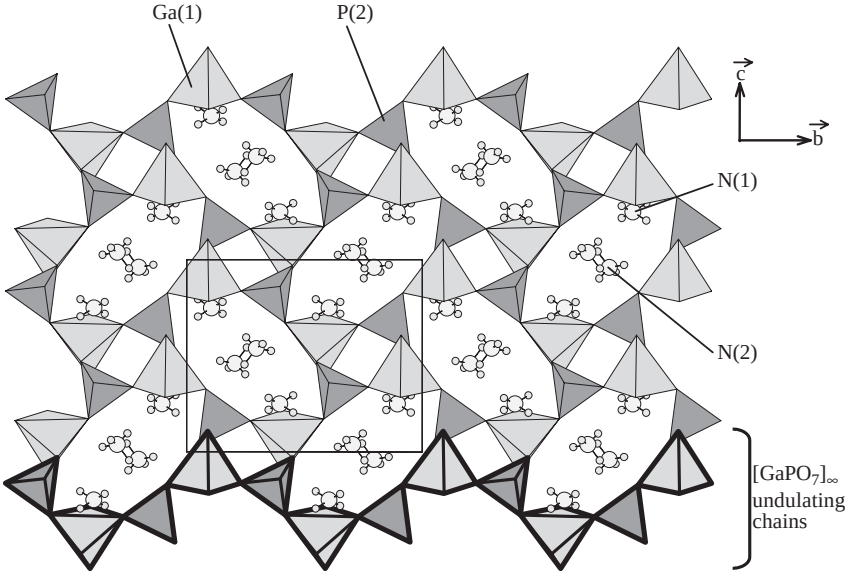

Fig. 4. Projection of the structure of the $[Ga_2P_2O_{10}]_\infty$ layer parallel to the $(\vec{b},\vec{c})$ plane, showing the $[GaPO_7]_\infty$ chains running along $\vec{b}$.

are located in the tunnels in two different sites. The NH_4^+ cation labelled N(2) adopts a slightly distorted tetrahedral geometry, with an average N(2)–H distance 0.83 Å and an average H–N(2)–H angle of 109°. The N(1) ammonium group geometry is much more distorted but the average values are approximately the same (0.82 Å and 110°). The positions of the hydrogen atoms (Fig. 5) of the NH_4^+ cations are closely correlated to the oxygen atoms surrounding each NH_4^+ cation, so that NH···O hydrogen bonds are formed. We indeed observe that the hydrogen atoms are pointing toward the closest oxygen atoms. As a result, each NH_4^+ cation N(1) is surrounded by eight oxygen atoms at distances ranging from 2.822 to 3.382 Å, and forms at least strong hydrogen bonds with two of them (Fig. 5a). Similarly, the NH_4^+ cation N(2) is surrounded by eight oxygen atoms at distances ranging from 2.741 to 3.275 Å and forms strong hydrogen bonds with four of them (Fig. 5b). The bond valence sum calculations [10] reported in Table 4 confirms the existence of these strong NH···O bonds: the four oxygen atoms O(2), O(4), O(5) and O(6) exhibit indeed a significant deviation from their expected valency. The NH···O angles range from 154° to 168°, deviating from 180° because of the presence of non boundary orbitals of oxygen atoms.

The analysis of the arrangement of the NH_4^+ cations in the structure is of interest. The latter form indeed rows of edge-sharing distorted $(NH_4)_4$ tetrahedra (N(2) sites) running along $\vec{c}$ (Fig. 6a) whose center is occupied by another NH_4^+ cation (N(1) sites). The relative disposition of these rows of [N(1)–(N(2))$_4$] tetrahedra (Fig. 6b) shows that the N(2)–N(2) distances between two adjacent chains is about of 3.6 Å, whereas the N(1)–N(2) distances are of 3.6 and 3.75 Å, suggesting that NH···N hydrogen bonds may also be formed. Thus the existence of numerous hydrogen bonds, due to the presence of NH_4^+ ions, may play a role in the stability of this microporous framework.

Attempts to prepare Rb and Cs analogs $A_3Ga_2(PO_4)_3$ (A = Rb, Cs) were unsuccessful. Nevertheless a partial substitution is possible, since we synthesized the phosphates $(NH_4)_{3-x}A_xGa_2(PO_4)_3$ with $0 \leqslant x \leqslant 0.23$ for A = Rb and $0 \leqslant x \leqslant 0.54$ for A = Cs. The structure refinements were carried out from several single crystal studies. As stated above, the atomic coordinates of the $[Ga_2P_3O_{12}]_\infty$ framework (Table 1) do not vary significantly with respect to $(NH_4)_3Ga_2(PO_4)_3$. The interatomic distances for the $x = 0.54$ Cs-phase and for the $x = 0.23$ Rb-phase are listed in Table 3. The geometry and distances are very similar in these phosphates compared to the pure ammonium phase. One only observes that the size of the GaO_5 and PO_4 polyhedra is slightly larger for $(NH_4)_{2.46}Cs_{0.54}Ga_2(PO_4)_3$ than for $(NH_4)_3Ga_2(PO_4)_3$ and for $(NH_4)_{2.77}Rb_{0.23}Ga_2(PO_4)_3$. More importantly, it is observed that the Rb^+ and Cs^+ cations sit only in the N(1) site (Table 1), the N(2) site being exclusively occupied by NH_4^+. This shows that the maximum occupancy level of the ammonium sites by rubidium or cesium should correspond to $x = 1$ and it suggests that the two NH_4^+ cations of the N(2) sites play a particular role in the stability of the structure, in agreement with the values of the N(2)–N(2) and N(2)–O distances.

Based on the latter remark, we have analyzed the structures of gallium phosphates containing NH_4^+ cations reported in literature. Our attention was drawn on the ammonium gallophosphates $NH_4[MGa_2(PO_4)_3(H_2O)_2]$ with M= Co, Mn [7,8]. The latter structure was described by Chippindale et al. [7,8] as a microporous

Table 3
Selected bond distances (Å) and angles (deg) in: (a) $(NH_4)_3Ga_2(PO_4)_3$; (b) $Rb_{0.23}(NH_4)_{2.77}Ga_2(PO_4)_3$; (c) $Cs_{0.54}(NH_4)_{2.46}Ga_2(PO_4)_3$; (d) $(NH_4)Ga_2Co(PO_4)_3 \cdot 2H_2O$

	(a)	(b)	(c)	(d)
Ga(1)–O(1)	1.8382(10)	1.8394(10)	1.8471(16)	1.840(3)
Ga(1)–O(2)	1.8503(10)	1.8496(10)	1.8575(16)	1.860(4)
Ga(1)–O(3)	1.8490(9)	1.8510(8)	1.8550(13)	1.857(3)
Ga(1)–O(4)	1.9878(13)	1.9857(13)	1.9865(19)	1.962(3)
Ga(1)–O(5)	1.9849(13)	1.9866(13)	1.9870(19)	2.014(3)
P(1)–O(3^{i})	1.5437(10)	1.5426(10)	1.5389(16)	1.523(4)
P(1)–O(3^{ii})	1.5437(10)	1.5426(10)	1.5389(16)	1.523(4)
P(1)–O(5)	1.5343(12)	1.5315(12)	1.5412(18)	1.540(3)
P(1)–O(5^{iii})	1.5343(12)	1.5315(12)	1.5312(18)	1.540(3)
P(2)–O(1^{iv})	1.5436(11)	1.5446(11)	1.5469(18)	1.537(4)
P(2)–O(2^{v})	1.5519(10)	1.5507(10)	1.5549(15)	1.542(4)
P(2)–O(4vi)	1.5328(12)	1.5324(13)	1.5333(19)	1.541(4)
P(2)–O(6)	1.5119(13)	1.5121(13)	1.5120(19)	1.511(4)
N(1)–H(1a)	0.94(3)			
N(1)–H(1a^{vii})	0.94(3)			
N(1)–H(1b)	0.70(3)			
N(1)–H(1b^{vii})	0.70(3)			
H(1a)–N(1)–H(1a^{vii})	103(3)			
H(1a)–N(1)–H(1b)	134(3)			
H(1a)–N(1)–H(1b^{vii})	99(3)			
H(1a^{vii})–N(1)–H(1b)	99(3)			
H(1a^{vii})–N(1)–H(1b^{vii})	134(3)			
H(1b)–N(1)–H(1b^{vii})	93(3)			
N(1)–O(3^{viii})	3.382(9)	3.2558(14)	3.2077(17)	
N(1)–O(3^{ix})	3.382(9)	3.2558(14)	3.2077(17)	
N(1)–O(4)	3.2416(10)	3.2537(9)	3.2894(14)	
N(1)–O(4^{vii})	3.2416(10)	3.2537(9)	3.2894(14)	
N(1)–O(6^{x})	2.822(3)	2.9364(16)	3.047(2)	
N(1)–O(6^{xi})	2.822(3)	2.9364(16)	3.047(2)	
N(1)–O(6^{v})	3.2797(12)	3.2764(13)	3.2807(18)	
N(1)–O(6^{xii})	3.2797(12)	3.2764(13)	3.2807(18)	
O(6^{x})–H(1a)–N(1)	163(3)			
N(2)–H(2a)	0.92(3)	0.95(3)	0.84(4)	
N(2)–H(2b)	0.82(3)	0.69(3)	0.93(4)	
N(2)–H(2c)	0.70(3)	1.08(3)	0.96(4)	
N(2)–H(2d)	0.88(3)	0.86(3)	0.81(4)	
H(2a)–N(2)–H(2b)	111(3)	119(3)	103(4)	
H(2a)–N(2)–H(2c)	113(3)	109(2)	113(3)	
H(2a)–N(2)–H(2d)	112(3)	109(3)	115(4)	
H(2b)–N(2)–H(2c)	112(4)	101(4)	118(4)	
H(2b)–N(2)–H(2d)	110(2)	114(3)	96(4)	
H(2c)–N(2)–H(2d)	99(3)	103(3)	111(4)	
N(2)–O(1^{xii})	3.2753(17)	3.2638(16)	3.276(3)	
N(2)–O(2^{iv})	3.193(2)	3.178(2)	3.158(3)	
N(2)–O(2^{ii})	2.9147(18)	2.9133(17)	2.920(3)	
N(2)–O(4^{iv})	3.0094(19)	3.0147(18)	3.020(3)	
N(2)–O(5)	2.9591(19)	2.9440(19)	2.942(3)	
N(2)–O(5^{iii})	3.2611(18)	3.2625(17)	3.270(3)	
N(2)–O(6^{xiii})	2.741(2)	2.7365(19)	2.734(3)	
N(2)–O(6^{xiv})	2.996(2)	2.979(2)	2.963(3)	

Table 3 (*continued*)

	(a)	(b)	(c)	(d)
O(6^{xiii})–H(2a)–N(2)	168(3)	158(3)	166(4)	
O(4^{iv})–H(2b)–N(2)	165(3)	157(4)	175(3)	
O(5)–H(2c)–N(2)	161(3)	154(3)	153(4)	
O(2^{ii})–H(2d)–N(2)	154(3)	161(4)	149(4)	

Symmetry codes: (i) $1-x$; $-y$; $1-z$; (ii) $\frac{1}{2}+x$; $\frac{1}{2}-y$;$-\frac{1}{2}+z$; (iii) $1+x$;$-y$; $\frac{1}{2}+z$; (iv) $\frac{1}{2}+x$; $\frac{1}{2}-y$; $\frac{1}{2}+z$; (v) $-x$; $1-y$;$-z$; (vi) $\frac{1}{2}+x$; $\frac{3}{2}-y$; $-\frac{1}{2}+z$; (vii) x; $-y$; $\frac{1}{2}+z$; (viii) $\frac{1}{2}-x$; $\frac{1}{2}-y$; $1-z$; (ix) $-1+x$;$-y$;$-\frac{1}{2}+z$; (x) $-x$; $-1-y$; $-z$; (xi) x; $-1-y$; $\frac{1}{2}+z$; (xii) $\frac{1}{2}-x$; $\frac{1}{2}-y$; $-z$; (xiii) $\frac{1}{2}-x$; $-\frac{1}{2}-y$; $-z$; (xiv) $\frac{1}{2}+x$; $-\frac{1}{2}-y$; $\frac{1}{2}+z$.

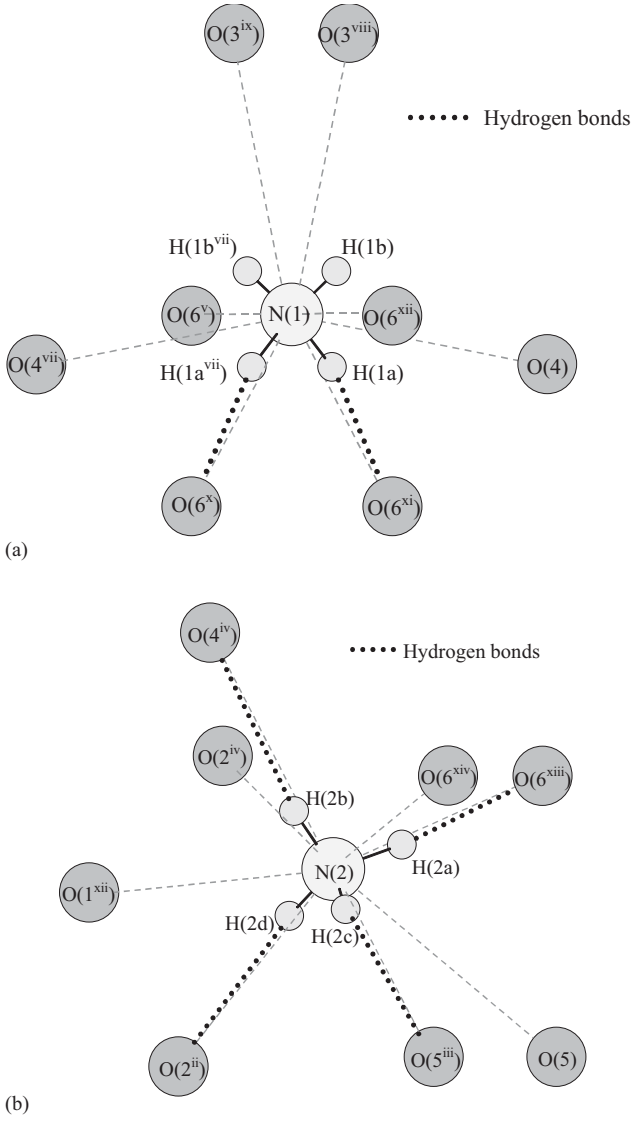

Fig. 5. Environment of the NH_4^+ cations by oxygen atoms showing the NH···O hydrogen bonds for N(1) (a) and N(2) (b).

3D framework of GaO_5, CoO_6 and PO_4 polyhedra forming tunnels where the NH_4^+ cations sit. In fact, one observes that the cell parameters of these two isotypic phosphates ($a = 13.323(3)$, $b = 10.245(1)$, $c = 8.886(2)$, $\beta = 108.43(2)$ for $NH_4[CoGa_2(PO_4)_3(H_2O)_2]$ and $a = 13.543(4)$, $b = 10.2302(15)$, $c = 8.894(3)$, $\beta = 108.54(3)$ for $NH_4[MnGa_2(PO_4)_3(H_2O)_2]$) are close to those of

Table 4
Electrostatic valence distribution for gallium, phosphorus and oxygen atoms in $(NH_4)_3Ga_2(PO_4)_3$

	Ga(1)	P(1)	P(2)	$\sum v_i-$
O(1)	0.75		1.18	1.92
O(2)	0.72		1.15	1.87
O(3)	0.72	1.18		1.90
		1.18		
O(4)	0.50		1.21	1.71
O(5)	0.50	1.21		1.71
		1.21		
O(6)			1.28	1.28
$\sum v_i+$	3.19	4.77	4.82	

$(NH_4)_3Ga_2(PO_4)_3$ [6]. Moreover, the atomic coordinates of Ga, P and O in these phosphates are similar to those observed for $(NH_4)_3Ga_2(PO_4)_3$. Consequently, the $[Ga_2P_3O_{12}]_\infty$ framework of the ammonium cobalt (or manganese) gallophosphates $NH_4[MGa_2(PO_4)_3(H_2O)_2]$ is practically identical to that described for $(NH_4)_3Ga_2(PO_4)_3$. The interatomic distances (Table 3) observed for the Co phase, e.g., are very similar to those of $(NH_4)_3Ga_2(PO_4)_3$. The GaO_5 bipyramids are slightly more distorted with two apical Ga–O distances of 1.962–2.014 instead of 1.984–1.987 Å, and three equatorial equivalent distances 1.840–1.857 instead of 1.838–1.849 Å. The P(1) tetrahedra are very regular with P–O distances ranging from 1.523 to 1.540 Å, similarly to 3D-GAPON (1.534–1.544 Å), whereas the P(2) tetrahedra exhibit one shorter bond (1.511 Å) linked to cobalt and three longer ones (1.537–1.542 Å) linked to gallium. Those bonds are very close to those observed for 3D-GAPON (1.512 and 1.533–1.552 Å, respectively). Note however that the shorter P–O bond in 3D-GAPON corresponds to a free apex whereas it is linked to cobalt (or manganese) in the latter phase. The NH_4^+ cation sits in the N(1) site with very similar N–O distances, ranging from 2.96 to 3.19 Å. The only main difference between these $(NH_4)MGa_2(PO_4)_3 \cdot 2H_2O$ phases and $(NH_4)_3Ga_2(PO_4)_3$ deals with the fact that in the N(2) site, the NH_4^+ cations are replaced by H_2O molecules and, in counterpart, cobalt (or manganese) is indeed inserted between the free apices of two adjacent P(2) tetrahedra (Fig. 7), forming two Co–O (or Mn–O) bonds with the latter and two Co–O (or Mn–O) longer bonds with the oxygen atoms (corresponding to O(5) in

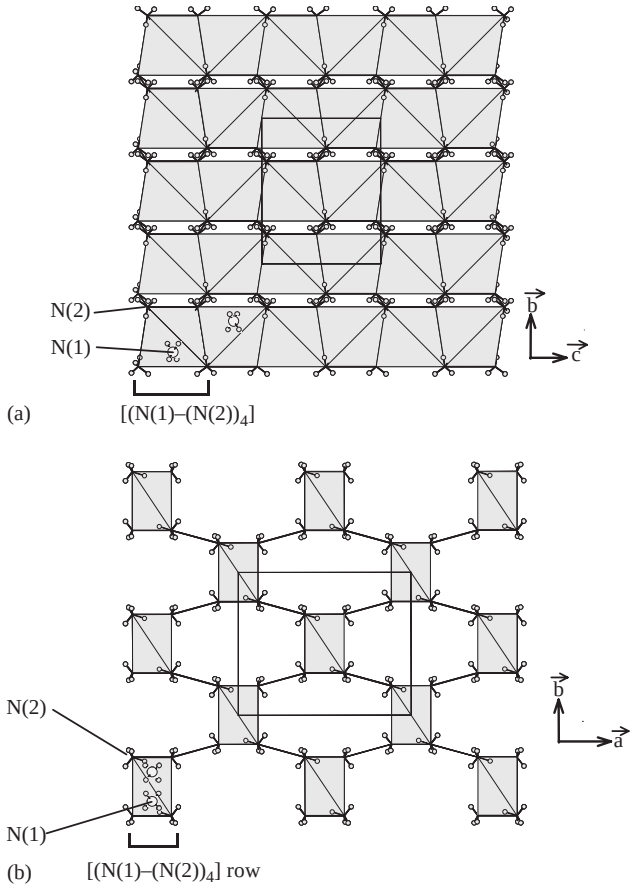

Fig. 6. The arrangement of NH_4^+ cations in $(NH_4)_3Ga_2(PO_4)_3$: (a) rows of edge-sharing $[N(1)–(N(2))_4]$ tetrahedra running along $\vec{c}$; the location of N(1) inside the $(N(2))_4$ tetrahedra is shown only for two of the $(N(2))_4$ tetrahedra. (b) Projection of the lattice of $[N(1)–(N(2))_4]$ tetrahedra along $\vec{c}$.

$(NH_4)_3Ga_2(PO_4)_3$) shared by the P(1) tetrahedra and the GaO_5 bipyramids. The octahedral coordination of cobalt (or manganese) is then completed by the two additional H_2O molecules located in the N(2) site. Thus, in these phosphates, Co^{2+} or Mn^{2+} reinforces the stability of the 3D $[Ga_2(PO_4)_3]_\infty$ framework, compensating the absence of the NH_4^+ cations in the N(2) sites. Note that the $[Ga_2(PO_4)_3]_\infty$ host lattice can also be stabilized without ammonium cation, as shown from the existence of the manganese gallophosphate $Mn_3(H_2O)_6Ga_4(PO_4)_6$ [11].

In conclusion, this structural investigation shows the great ability of the three-dimensional $[Ga_2(PO_4)_3]_\infty$ anionic framework to accommodate, besides NH_4^+ cations, various species such as Rb^+ or Cs^+ cations, but also Co^{2+} or Mn^{2+} as hydrated cations, i.e., $[Co(H_2O)_2]^{2+}$ or $[Mn(H_2O)_2]^{2+}$. Remarkably, the geometry of this framework, due to its microporous character, is not significantly modified by the nature of the interpolated species. Further investigations should allow numerous other ions or molecules to be inserted in this intersecting tunnel structure.

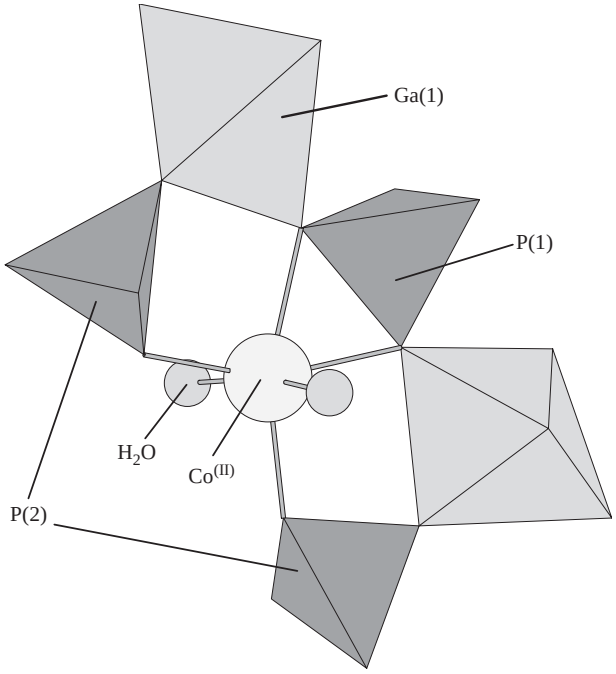

Fig. 7. Connection of the $CoO_4(H_2O)_2$ octahedron with the P(1), P(2) tetrahedra and with the GaO_5 pyramids in the $(NH_4)[Co(H_2O)_2]Ga_2(PO_4)_3$ structure.

Acknowledgments

The authors wish to thank the Grant Agency of the Czech Republic (Grant 202/03/0430). The authors also gratefully acknowledge the Région Basse Normandie and the Ministère de la Recherche for financial support.

References

[1] A.K. Cheetham, G. Férey, T. Loiseau, Angew. Chem. Int. Ed. 38 (1999) 3268.
[2] C. Sassoye, T. Loiseau, F. Tantelle, G. Ferey, Chem. Commun. (2000) 943.
[3] E. Estermann, L.B. McCuster, C. Baerlocker, A. Merrouche, H. Kessler, Nature 352 (1991) 320.
[4] C.H. Lin, S.L. Wang, K.H. Lii, J. Am. Chem. Soc. 123 (2001) 4649.
[5] M. Mertens, C. Schott-Darie, P. Reinert, J.L. Guth, Microporous Mater. 5 (1995) 91.
[6] F. Bonhomme, S.G. Thoma, T.M. Nenoff, Microporous Mater. 53 (2002) 87.
[7] A.M. Chippindale, A.R. Cowley, R.I. Walton, J. Mater. Chem. 6 (1996) 611.
[8] A.M. Chippindale, A.R. Cowley, A.D. Bond, Acta Crystallogr. C 59 (2003).
[9] V. Petricek, M. Dusek, The crystallographic computing system JANA2000, Institute of Physics, Praha, Czech Republic, 2000.
[10] N.E. Brese, M. O'Keeffe, Acta Crystallogr. B 47 (1991) 192–197.
[11] K.F. Hsu, S.L. Wang, Inorg. Chem. 39 (2000) 1773–1778.